In Situ FTIR ATR Spectroscopy of the Preparation of an Oriented Monomolecular Film of Porin Omp32 on an Internal Reflecting Element by Dialysis

Michael Schwarzott,[†] Harald Engelhardt,[‡] Thomas Klühspies,[‡] Dieter Baurecht,[†] Dieter Naumann,[§] and Urs P. Fringeli*[,†]

Institute of Physical Chemistry, University of Vienna, Althanstrasse 14, A-1090 Vienna, Austria, Max-Planck Institut für Biochemie, Am Klopferspitz 18, W-8033 Martinsried, Germany, and Robert Koch-Institut, P34, Nordufer 20, 13353 Berlin, Germany

Received January 29, 2003. In Final Form: June 4, 2003

The development of a reproducible technique for the preparation of oriented porin Omp32 monolayers on an attenuated total reflection (ATR) internal reflection element (IRE) was the principal aim of this work. A procedure earlier applied for two-dimensional crystallization of membrane proteins [Paul, A.; Engelhardt, H.; Jakubowski, U.; Baumeister, W. *Biophys. J.* **1992**, *61*, 172−188] could be successfully adapted. Layer formation was performed in a spectroscopic dialysis cell in the presence of 1,2-dimyristoyl-*sn*-glycero-3-phosphocholine (DMPC) micelles by the removal of the detergent (*n*-octylpolyoxyethylene, OPOE). This setup enabled in situ monitoring of the monolayer formation by means of the Fourier transform infrared (FTIR) single beam sample reference ATR technique. The time course of OPOE and sodium azide extraction by dialysis and the formation of the protein/lipid layer on top of the IRE was evaluated from corresponding time-dependent absorbance changes in the IR spectra. Both OPOE and azide featured a first-order kinetics, whereas the synchronous adsorption of porin to the Ge IRE resulted in a sigmoidal time behavior. At the beginning of the dialysis, the concentration of OPOE was just above the critical micellar concentration (cmc) which is about 0.25%. As the cmc was reached by dialysis, Omp32 adsorption was accelerated, reaching saturation after about 5 h. Quantitative analysis of the Omp32/lipid layer gave strong evidence for a well-ordered monolayer with the barrel axis of the Omp32 trimer being approximately oriented perpendicular to the supporting IRE. Two to six DMPC molecules were detected per Omp32 monomer.

Introduction

Gram-negative bacteria are characterized by an outer membrane which serves as an effective protection against noxious compounds. The uptake of nutrients and ions is enabled by the outer membrane proteins referred to as porins. Porins are divided into two classes, the unspecific or general porins, which build up unspecific diffusion pores, and those which form substrate-specific channels (for reviews, see refs 1−3). The general porins allow the transport of solutes up to a molecular mass of ∼600 Da by passive diffusion,[4] but they often show a selectivity to either cations or anions, for example, OmpF and PhoE of *Escherichia coli*.[5] The Omp32 from *Delftia acidovorans* (formerly *Comamonas acidovorans*) is a strongly anion selective porin.[6] The three-dimensional structure was recently determined by X-ray crystallography at 0.21 nm resolution.[7] As is typical for bacterial outer membrane proteins, Omp32 has a β-barrel structure. A monomer is built up of 16 amphipathic antiparallel β strands connected by seven short periplasmic and eight external loops resulting in a molecular mass of 34.7 kDa. Each monomer of Omp32 forms a complex with a 5.8 kDa peptide. Porin and peptide together form a funnel-like homotrimer where the peptides are located close to the trimer axis at the periplasmic side. It is assumed that the peptides are involved in linking the outer membrane with the cell wall peptidoglycan.[7] One of the external loops (L3) folds back into the center of the channel and determines together with a small protrusion (P1 of β strand β2) a particularly narrow constriction zone. A cluster of three charged arginine residues in this constriction in conjunction with further arginine and lysine residues at the external and periplasmic pore entrances creates a large positive electric potential within the channel.[8] This is suggested to represent the selectivity filter of the porin. Omp32 shows voltage-dependent closing when incorporated in planar lipid bilayers.[6] This kind of voltage gating means the enhanced probability of closed states of porin channels when a positive or negative electric potential exceeding a certain threshold value is applied. This gating phenomenon appears to be a general feature of β-barrel outer membrane proteins (for reviews, see refs 9 and 10). A recent study has shown the influence of charged amino acids within the constriction zone of OmpF on voltage sensing and conductance.[11] It was found that an increase

* To whom correspondence should be addressed. Phone: +43-1-4277 525 30. Fax: +43-1-4277 9525. E-mail: urs.peter.fringeli@univie.ac.at.

[†] University of Vienna.

[‡] Max-Planck Institut für Biochemie.

[§] Robert Koch-Institut.

(1) Koebnik, R.; Locher, K. P.; Van Gelder, P. *Mol. Microbiol.* **2000**, *37*, 239−253.

(2) Schirmer, T. J. *J. Struct. Biol.* **1998**, *121*, 101−109.

(3) Schulz, G. E. *Curr. Opin. Struct. Biol.* **1996**, *6*, 485−490.

(4) Jap, B. K.; Walian, P. J. *Physiol. Rev.* **1996**, *76*, 1073−1088.

(5) Van Gelder, P.; Saint, N.; Phale, P.; Eppens, E. F.; Prilipov, A.; van Boxtel, R.; Rosenbusch, J. P.; Tommassen, J. *J. Mol. Biol.* **1997**, *269*, 468−472.

(6) Mathes, A.; Engelhardt, H. *Biophys. J.* **1998**, *75*, 1255−1262.

(7) Zeth, K.; Diederichs, K.; Welte, W.; Engelhardt, H. *Structure* **2000**, *8*, 981−992.

(8) Zachariae, U.; Koumanov, A.; Engelhardt, H.; Karshikoff, A. *Protein Sci.* **2002**, *11*, 1309−1319.

(9) Delcour, A. H. *FEMS Microbiol. Lett.* **1997**, *151*, 115−123.

(10) Bainbridge, G.; Gokce, I.; Lakey, J. H. *FEBS Lett.* **1998**, *431*, 305−308.

(11) Phale, P. S.; Philippsen, A.; Widmer, C.; Phale, V. P.; Rosenbusch, J. P.; Schirmer, T. *Biochemistry* **2001**, *40*, 6319−6325.

10.1021/la034153m CCC: $25.00
Published on Web 07/23/2003

in the charge density increases the ion flow, whereas the effects on voltage gating could not be correlated with the charge state of the pore constriction. Conformational changes of extracellular loops of OmpF in response to an applied electric potential, which led to an occlusion of the pore entrance, were observed by atomic force microscopy measurements.[12] This possible mechanism of voltage gating would be supported by a study of channel conductance in a planar lipid bilayer of a porin from *Haemophilus influenza* type b, where single mutations of amino acids in an extracellular loop had changed the threshold value for channel closing.[13] To verify this mechanism, an experimental approach is required, which is able to monitor conformational changes. Attenuated total reflection (ATR) Fourier transform infrared (FTIR) difference spectroscopic methods are capable of detecting changes in protein structure. Moreover, modulation spectroscopy enables access to a kinetic analysis of the sample response of a varying external parameter (e.g., electric field).[14] However, independently of the chosen ATR FTIR method, it is a prerequisite to achieve a reproducible technique of protein immobilization on the internal reflection element (IRE).

In this paper, we present a method for Omp32 monolayer preparation which was adapted from two-dimensional crystallization of membrane proteins in the presence of phospholipids, as used for example earlier for sample preparation in electron microscopy. As a consequence of slow removal of the detergent from a mixture of solubilized porin and lipid micelles by dialysis, the protein reconstituted into the lipid matrix. It formed layers with different symmetries and dimensions of the unit cell, depending on the experimental conditions applied. Relevant parameters turned out to be the lipid-to-protein ratio, the temperature, and the nature of lipids or detergents.[15,16] We have used an ATR flow-through dialysis cell which allowed dialysis of the Omp32 and 1,2-dimyristoyl-*sn*-glycero-3-phosphocholine (DMPC) suspension, monitoring the process in situ by FTIR ATR spectroscopy. Our conditions were similar to those described in ref 17.

Materials and Methods

Materials. DMPC was purchased from Fluka Chemie GmbH (Buchs, Switzerland), deuterium-labeled 1,2-dimyristoyl-d67-*sn*-glycero-3-phosphocholine (DM-d67-PC, all protons except the five from the glycerol part exchanged, deuterium purity >98%) from Avanti Polar Lipids, Inc. (Alabaster, AL), and *n*-octylpolyoxyethylene ($n = 2-9$, OPOE) from Bachem AG (Bubendorf, Switzerland). Other chemicals were of analytical grade and obtained from Fluka Chemie GmbH. All chemicals were used without further purification. Porin Omp32 was extracted by means of OPOE from outer membranes of *D. acidovorans* (Deutsche Sammlung von Mikroorganismen und Zellen, DSMZ, no. 39) as described in detail in ref 18. The outer membrane protein was stored in 10 mM phosphate buffer, pH 7.4, containing 150 mM NaCl, 3 mM NaN_3, and about 0.5% OPOE.

The concentration of solvated Omp32 was determined via UV absorption at 278 nm on a Zeiss Specord UV/VIS S10 using a calibration curve of bovine serum albumin (BSA) at concentrations between 0.03 and 1.0 mg/mL. OPOE and NaN_3 additives did not disturb.

FTIR ATR Spectroscopy. A Bruker IFS-66 FTIR spectrometer (Ettlingen, Germany) with a "lift-model" single beam sample reference (SBSR) mirror attachment[19] (OPTISPEC, CH-8173 Neerach, Switzerland) was used. The attachment was equipped with a rotatable polarizer, consisting of 0.12 μm wide strips of aluminum on a KRS-5 substrate (SPECAC, Orpington, U.K.) and a liquid nitrogen cooled mercury-cadmium-telluride (MCT) detector. In SBSR measurements, the infrared beam propagates alternately through the upper and lower half of the IRE with a short mutual time delay. One-half of the ATR multiple IRE is used for the sample (S), and the other one for the reference (R). SBSR absorbance spectra are calculated from corresponding single channel spectra recorded with the IR beam passing through the sample side and the reference side of the IRE, respectively. All spectra were scanned at 4 cm^{-1} resolution with a zero filling factor of 4 and a Blackman Harris 3 term apodization. The spectrometer was purged with dry and carbon dioxide free air. A germanium trapezoid ($54 \times 30 \times 1.5$ mm^3) with an angle of incidence $\theta = 45°$ was used as the IRE. The mean number of active internal reflections in the IRE was $N = 14.1$ throughout all experiments. Spectra were recorded with parallel (pp) and perpendicular polarized (vp) incident infrared light, and 500−1000 scans were accumulated to achieve the desired signal-to-noise ratio. The IRE (Ge plate) was polished by means of 0.25 μm diamond paste on a pellon cloth (Logitech Ltd., Old Kilpatrick, Scotland) PM5 polishing machine. Before use, the IRE was cleaned for 3 min by plasma (Harrick Sci. Corp., Ossining, NY). The sample and reference regions of the IRE were encapsulated by flow through cuvettes made of Delrin. Each chamber featuring a volume of about 100 μL was connected via Ismapren tubes to an external peristaltic pump. The hole cell was thermostated by means of external circulating water. A SBSR dialysis cell was used (OPTISPEC, CH-8173 Neerach, Switzerland) featuring an inner compartment of approximately 100 μL volume, which was bordered by the IRE and the dialysis membrane, while the outer compartment with the same volume was bordered by the dialysis membrane and the cell back-wall. Both compartments are hydrodynamically optimized for flow-though. In this experiment, the dialysis membrane had a pore size of 5 kDa (Messinger Membrane Systems AG, Zürich, Switzerland).

Dialysis. An aliquot of a solution of DMPC or DM-d67-PC in chloroform was dried in a nitrogen stream and then dissolved in the Omp32 buffer solution by vortexing. The solution contained 4 ± 1 mg/mL Omp32 (0.1 ± 0.025 mmol/L calculated with a molar mass of 40.5 kDa). This mixture of detergent-solubilized porin and lipid with a lipid-to-protein ratio (L/P) (mol/mol) of 9.2 $\pm$ 2.3 (DMPC) and of 8.3 $\pm$ 2.1 (mol/mol) (DM-d67-PC), respectively, was filled into the inner compartment of the sample side of the dialysis cell. This compartment is in direct contact with the IRE. Then the tubes at the inlet and outlet were clamped at the entrance of the cell. The temperature of the cell was set to 35 ± 0.5 °C, that is, well above the transition temperature of DMPC (~24 °C from ref 20). A 10 mM phosphate buffer, pH 7.4, containing 150 mM NaCl was used as the dialysis buffer and was filled into the reference side of the cell. The buffer was degassed and thermostated before it was pumped through the outer chamber of the sample side of the dialysis cell. The pump speed of the dialysate was 0.28 mL/min. SBSR absorbance spectra were recorded in situ during the dialysis process, which was stopped when no additional spectral changes were noticeable within at least 1 h of observation. A SBSR background spectrum of the phosphate buffer filled into both the sample and the reference compartments of the dialysis cell was subtracted from all SBSR spectra in order to get enhanced background compensation by compensating inhomogeneities resulting predominantly from the IRE and the sensitive area of the MCT detector element.

H/D Exchange. After porin had adsorbed onto the Ge IRE, the temperature of the dialysis cell was reduced to 23 ± 0.5 °C

(12) Müller, D. J.; Engel, A. *J. Mol. Biol.* **1999**, *285*, 1347−1351.
(13) Arbing, M. A.; Hanrahan, J. W.; Coulton, J. W. *Biochemistry* **2001**, *40*, 14621−14628.
(14) Baurecht, D.; Fringeli, U. P. *Rev. Sci. Instrum.* **2001**, *72*, 3782−3792.
(15) Engel, A.; Hoenger, A.; Hefti, A.; Henn, C.; Ford, R. C.; Kistler, J.; Zulauf, M. *J. Struct. Biol.* **1992**, *109*, 219−234.
(16) Jap, B. K.; Zulauf, M.; Scheybani, T.; Hefti, A.; Baumeister, W.; Aebi, U.; Engel, A. *Ultramicroscopy* **1992**, *46*, 45−84.
(17) Paul, A.; Engelhardt, H.; Jakubowski, U.; Baumeister, W. *Biophys. J.* **1992**, *61*, 172−188.
(18) Zeth, K.; Schnaible, V.; Przybylski, M.; Welte, W.; Diederichs, K.; Engelhardt, H. *Acta Crystallogr.* **1998**, *D54*, 650−653.
(19) Fringeli, U. P. In *Encyclopedia of Spectroscopy and Spectrometry*; Lindon, J. C., Tranter, G. E., Holmes, J. C., Eds.; Academic Press: San Diego, 2000; pp 58−75.
(20) Blume, A. *Biochemistry* **1983**, *22*, 5436−5442.

Table 1. Optical and Spectroscopic Parameters for Quantification of the Surface Concentration of Omp32, DMPC, and DM-d67-PC

	Omp32, amide I′	Omp32, ν(NH)	DMPC, $\nu_s(CH_2)$	DM-d67-PC, $\nu_s(CD_2)$
n_1[a]	4.0 ± 0	4.0 ± 0	4.0 ± 0	4.0 ± 0
n_2[b]	1.4 ± 0.06	1.4 ± 0.06	1.45 ± 0.06	1.45 ± 0.06
n_3[c]	1.32 ± 0.06	1.27 ± 0.06	1.22 ± 0.06	1.38 ± 0.06
θ/deg[d]	45 ± 1.5	45 ± 1.5	45 ± 1.5	45 ± 1.5
$\int\epsilon(\tilde{\nu})\,d\tilde{\nu}$/(cm·mol^{-1})[e]	$2.74 \times 10^7 \pm 3.0 \times 10^6$	$2.09 \times 10^7 \pm 2.2 \times 10^6$	$5.7 \times 10^5 \pm 2 \times 10^4$	$5.9 \times 10^5 \pm 1.0 \times 10^5$
$\Delta\tilde{\nu}$/cm^{-1} [f]	1706−1595	3400−3200	2869−2830	2131−2045
$\tilde{\nu}_{max}$/cm^{-1} [g]	1650	3280	2852	2093
ν[h]	384	384	28	26
N[i]	14.1 ± 1	14.1 ± 1	14.1 ± 1	14.1 ± 1

[a] Refractive index of Ge IRE. [b] Refractive index of the sample film. [c] Refractive index of the bulk water (D_2O). [d] Angle of incidence. [e] Integrated decadic molar absorption coefficient. [f] Range of integration. [g] Wavenumber of absorption maximum. [h] Number of equivalent functional groups per molecule. [i] Number of active internal reflections.

(room temperature), the buffer was removed, and the dialysis cover of the cell was replaced by a standard SBSR flow-through cap. Both sides of the cell were refilled immediately with degassed buffer of room temperature, so that the porin film remained hydrated during this process. Then the buffer in both compartments (R and S) of the SBSR cell was replaced by 150 mM NaCl in D_2O, initiating the H/D exchange. Time-resolved measurements were started immediately after H_2O buffer replacement.

At the end of this experiment, the porin film was removed by means of a 0.3 M SDS solution containing 0.1 M EDTA to enable the measurement of background SBSR spectra in the D_2O environment.

Monofilm Preparation. To calculate the lipid coverage in the dialysis experiment, dry DMPC and DM-d67-PC monofilms were prepared on an IRE by means of the Langmuir−Blodgett (LB) technique as described for 1,2-dipalmitoyl-*sn*-glycero-3-phosphoric acid (DPPA)[21] by means of a film balance (Nima Technology Ltd., Science Park, Coventry, U.K.). The surface pressure was 30 ± 0.2 mN/m during film transfer at room temperature with a transfer rate of 2 mm/min. The subphase consisted of pure water containing 0.1 mM $CaCl_2$.

Data Analysis. Determination of the surface concentration of Omp32 and DMPC/DM-d67-PC was performed by means of equations derived with the thin film and weak absorber approximations as described in the theoretical section. Uniaxial orientation with the feature of liquid crystalline ultrastructure (LCU) was assumed for both adsorbed Omp32 and DMPC as well as DM-d67-PC, respectively. The thickness d of an adsorbed porin monolayer is estimated as $d = 44 \pm 5$ Å taking the three-dimensional structure of Omp32[7] and the electron density profiles of DMPC[22] into account. Since the penetration depth $d_p \geq 0.18$ μm, the condition of a thin film $d \ll d_p$ is fulfilled.

The optical parameters for Omp32 quantification were taken from ref 23 and are summarized in Table 1. The surface concentration of Omp32 was calculated from the integrated absorbance of the amide I′ band at 1650 cm^{-1}, that is, $\int A_{pp}(\tilde{\nu})\,d\tilde{\nu}$ for parallel and $\int A_{vp}(\tilde{\nu})\,d\tilde{\nu}$ for perpendicular polarized incident light using eq 9. To determine the amount of not-exchangeable amide protons, the ν(NH) band at 3280 cm^{-1} was integrated and analyzed, using parameters from ref 23 as indicated in Table 1. The number of amide groups per molecule was deduced from the Omp32 3D structure,[7] resulting in 332 amino acids for the porin monomer and 54 amino acids for the associated peptide. LB monolayers of DMPC and DM-d67-PC on a Ge IRE were used to determine integrated decadic molar absorption coefficients $\int\epsilon(\tilde{\nu})\,d\tilde{\nu}$ of the symmetric CD_2 stretching vibration ($\nu_s(CD_2)$) at 2093 cm^{-1} and the ester C═O stretching vibration at 1739 cm^{-1} (ν(C═O)). The latter was evaluated from a DMPC monolayer by calculating first its surface concentration via CH_2 stretching according to ref 24. Then $\int\epsilon(\tilde{\nu})\,d\tilde{\nu}$ of ν(C═O) could be determined as $7.2 \times 10^6 \pm 8 \times 10^5$ cm·mol^{-1} and was used for the calculation of the surface concentration of the DM-d67-PC LB layer. From this value, $\int\epsilon(\tilde{\nu})\,d\tilde{\nu}$ of $\nu_s(CD_2)$ at 2093 cm^{-1} was calculated; see Table 1. The anomalous dispersion of H_2O[25] and D_2O[26] at peak maxima of $\nu_s(CH_2)$ and $\nu_s(CD_2)$ was taken into account. Refractive indices of the aqueous environment n_3 were used as mean values within the integration ranges indicated in Table 1. All integrations were performed with a straight baseline drawn tangentially between the limits of integration.

Theoretical Section

Orientation Measurements. Orientation measurements require independent spectra of the sample by means of parallel and perpendicular polarized incident light. To get rid of physical and molecular constants, such as the magnitude of the transition moment, the so-called dichroic ratio $R(\tilde{\nu}) = \int A_{pp}(\tilde{\nu})\,d\tilde{\nu} / \int A_{vp}(\tilde{\nu})\,d\tilde{\nu}$ is generally used as basic quantity. $\int A_{pp}(\tilde{\nu})\,d\tilde{\nu}$ and $\int A_{vp}(\tilde{\nu})\,d\tilde{\nu}$ denote the integrated absorbances of measured spectra with parallel and perpendicular polarized incident light. Peak absorbances may also be used instead of integrated absorbances.

By means of the real parts of the refractive indices of the IRE, the thin film and the bulk medium, as well as the angle of incidence, one obtains the relative electric field components $E_x(\tilde{\nu})$, $E_y(\tilde{\nu})$, and $E_z(\tilde{\nu})$ at a distinct wavenumber of a thin film in contact with a bulk rarer medium according to Harrick's approximation of Fresnel's equations.[27,28] This so-called thin film approximation is valid when the film thickness is very small compared to the depth of penetration and in the case of a weakly absorbing sample.[29] Both conditions are fulfilled for a monomolecular layer of biological material. Assuming a LCU, that is, an uniaxial arrangement of the sample, one obtains for the dichroic ratio the following expression:

$$R = \frac{\int A_{pp}(\tilde{\nu})\,d\tilde{\nu}}{\int A_{vp}(\tilde{\nu})\,d\tilde{\nu}} = \frac{E_x^2}{E_y^2} + 2\frac{E_z^2\overline{\langle\cos^2\Theta\rangle}}{E_y^2(1 - \overline{\langle\cos^2\Theta\rangle})} \quad (1)$$

(Note that for the sake of simplicity, the dependence of the dichroic ratio and the relative electric field components on the wavenumber ($\tilde{\nu}$) is not explicitly indicated.)

$\overline{\langle\cos^2\Theta\rangle}$ denotes the average over the mean squares of the cosines of the angles between the transition moments of a given vibration and the z-axis of the laboratory coordinate system, which is fixed to the IRE. The xy-plane

(21) Wenzl, P.; Fringeli, M.; Goette, J.; Fringeli, U. P. *Langmuir* **1994**, *10*, 4253−4264.
(22) Moore, P. B.; Lopez, C. F.; Klein, M. L. *Biophys. J.* **2001**, *81*, 2484−2494.
(23) Fringeli, U. P.; Apell, H.-J.; Fringeli, M.; Läuger, P. *Biochim. Biophys. Acta* **1989**, *984*, 301−312.
(24) Reiter, G.; Siam, M.; Falkenhagen, D.; Gollneritsch, W.; Baurecht, D.; Fringeli, U. P. *Langmuir* **2002**, *18*, 5761−5771.
(25) Bertie, J. E.; Lan, Z. *Appl. Spectrosc.* **1996**, *50*, 1047−1057.
(26) Bertie, J. E.; Ahmed, M. K. *J. Phys. Chem.* **1989**, *93*, 2210−2218.
(27) Fringeli, U. P. In *Internal Reflection Spectroscopy*; Mirabella, F. M., Ed.; Marcel Dekker: New York, 1992; pp 255−324.
(28) Harrick, N. J. *Internal Reflection Spectroscopy*; Harrick Sci. Corp.: Ossining, NY, 1979.
(29) Picard, F.; Buffeteau, T.; Desbat, B.; Auger, M.; Pézolet, M. *Biophys. J.* **1999**, *76*, 539−551.

is parallel to the surface of the IRE, and the *x*-axis is aligned along the direction of light propagation. The *z*-axis is perpendicular to the IRE surface.

Solving eq 1 for the mean square cosine results in

$$\overline{\langle\cos^2\Theta\rangle} = \frac{E_x^2 - RE_y^2}{E_x^2 - RE_y^2 - 2E_z^2} \tag{2}$$

Three special cases of molecular orientation should be mentioned here, the isotropic arrangement of transition dipole moments, resulting in $\langle\cos^2\Theta\rangle_{iso} = {}^1/_3$, the perfect alignment of the transition dipole moments parallel to the surface of the IRE (*xy*-plane), resulting in $\langle\cos^2\Theta\rangle_{xy} = 0$, and perfect alignment of transition moments along the normal to the IRE (*z*-axis), resulting in $\langle\cos^2\Theta\rangle_z = 1$, respectively. As can be derived from eq 1, the corresponding dichroic ratios are

$$R_{iso} = \frac{E_x^2 + E_z^2}{E_y^2} \qquad R_{xy} = \frac{E_x^2}{E_y^2} \qquad R_z = \infty \tag{3}$$

Dichroic difference spectra D^* offer a fast and easy way to get orientational information. A D^* spectrum is defined as the weighted difference spectrum between the absorbance spectra measured with parallel and perpendicular polarized incident light as given in eq 4.

$$D^*(\tilde{\nu}) = A_{pp}(\tilde{\nu}) - R_{iso}A_{vp}(\tilde{\nu}) \tag{4}$$

The weighting factor R_{iso} has to be calculated as shown above and denotes the dichroic ratio of an isotropic sample. Contrary to transmission spectroscopy, R_{iso} differs from unity and has to be calculated in each case depending on the optical constants of the sample.[23,30] Consequently, the dichroic difference spectrum as defined by eq 4 results in a horizontal line if the sample is isotropic or the respective mean transition moment assumes the so-called magic angle of $\langle\Theta\rangle = 54.74°$ (uniaxial orientation) with the axis normal to the IRE surface. A positive D^* band indicates predominant alignment of transition moments of a given vibration in the direction of the *z*-axis, that is, $\langle\Theta\rangle < 54.74°$, while a negative D^* band is significant for predominant alignment of the transition moments parallel to the reflecting surface of the IRE (*xy*-plane), that is, assuming a mean angle $\langle\Theta\rangle > 54.74°$ with the *z*-axis.

Determination of Surface Concentration. The volume concentration *c* and the surface concentration Γ are related to each other via the thickness of the sample *d* and Lambert−Beer's law by

$$c = \frac{\Gamma}{d} = \frac{\int A_{vp}(\tilde{\nu})\,d\tilde{\nu}}{N\nu d_{e,vp}\int \epsilon(\tilde{\nu})\,d\tilde{\nu}} \tag{5}$$

where, as before, $\int A_{vp}(\tilde{\nu})\,d\tilde{\nu}$ denotes the integrated absorbance of a distinct absorption band obtained by a measurement with perpendicular polarized light. *N* and *ν* are the mean number of the active internal reflections and the number of equal functional groups (e.g., amide groups) per molecule. $\int\epsilon(\tilde{\nu})\,d\tilde{\nu}$ denotes the decadic integrated molar absorption coefficient of this band. The effective thickness of an arbitrarily oriented sample per internal reflection is denoted by $d_{e,vp}$. It indicates the hypothetical sample thickness required for a transmission experiment in order to give the same absorbance as obtained with the real ATR measurement, thus enabling the use of Lambert−Beer's law for quantitative ATR spectroscopy. The corresponding analytical expressions for perpendicular and parallel polarized light are composed of the axial contributions which depend on the corresponding effective thickness of an isotropic sample as well as on the mean square cosine according to eqs 6 and 7:

$$d_{e,vp} = d_{e,y} = \frac{3}{2}(1 - \overline{\langle\cos^2\Theta\rangle})d_{e,y}^{iso} \tag{6}$$

$$d_{e,pp} = d_{e,x} + d_{e,z} = \frac{3}{2}(1 - \overline{\langle\cos^2\Theta\rangle})d_{e,x}^{iso} + 3\overline{\langle\cos^2\Theta\rangle}d_{e,z}^{iso} \tag{7}$$

According to Harrick's thin film approximation,[28] the axial effective thickness of an isotropic sample $d_{e,x}^{iso}$, $d_{e,y}^{iso}$, and $d_{e,z}^{iso}$, respectively, is proportional to the real sample thickness *d*, thus enabling the definition of the relative effective thickness, depending only on optical parameters.

$$d_{e,i}^{rel,iso} = \frac{d_{e,i}^{iso}}{d} = \frac{n_2}{n_1\cos\theta}E_i^2 \tag{8}$$

n_1 is the refractive index of the IRE, n_2 is the refractive index of the film, θ is the angle of incidence, and $i = x, y, z$, respectively.

Using the relative isotropic effective thickness $d_{e,vp}^{rel,iso} = d_{e,y}^{rel,iso}$ and inserting eq 2 for the mean square cosine $\langle\cos^2\Theta\rangle$, one obtains the following expression for the surface concentration of a substance in a thin film assuming a liquid crystalline ultrastructure:

$$\Gamma = \frac{\int A_{vp}(\tilde{\nu})\,d\tilde{\nu}}{3N\nu d_{e,vp}^{rel,iso}\int\epsilon(\tilde{\nu})\,d\tilde{\nu}}\left[2 - \frac{E_x^2}{E_z^2} + R\frac{E_y^2}{E_z^2}\right] \tag{9}$$

The surface concentration Γ as given in eq 9 may be understood as the projection of the molecules in the volume defined by the unit area and the height *d* (real sample thickness).

In a recent review article,[30] it was shown that eqs 1−9, which are based on the thin film and the weak absorber approximation, are in excellent agreement with straightforward accurate ATR data analysis even for many bulk organic and inorganic media.

Error Analysis. The uncertainties indicated in this paper are all based on a straightforward error propagation calculation.[31] Analytical expressions for partial derivatives have been evaluated by means of the Symbolic Mathematical Toolbox of MATLAB,[32] whereas the final numeric calculation of overall uncertainties has been performed by means of the standard MATLAB software. The uncertainties of the input parameters are presented in Table 1. They correspond to approximately a 95% limit of confidence.

Results

Preparation of Oriented Omp32/Lipid Layers. The mixture of Omp32 and deuterated DM-d67-PC (or DMPC

(30) Fringeli, U. P.; Baurecht, D.; Siam, M.; Reiter, G.; Schwarzott, M.; Bürgi, T.; Brüesch, P. ATR Spectroscopy of Thin Films. In *Handbook of Thin Films Materials*; Nalwa, H. S., Ed.; Academic Press: New York, 2002; Vol. 2, Chapter 4, pp 191−229.

(31) Zurmühl, R. *Praktische Mathematik für Ingenieure und Physiker*; Springer-Verlag: Berlin, 1965.

(32) The MathWorks, Inc., 24 Prime Park Way, Natick, MA 01760.

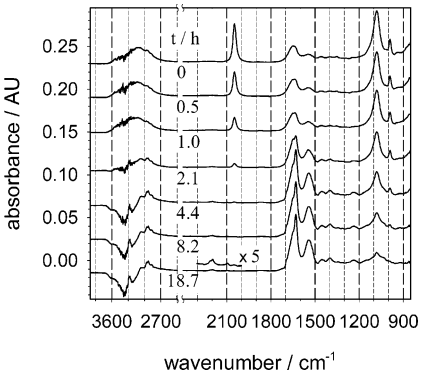

Figure 1. Time-resolved SBSR ATR FTIR spectra recorded in situ during the dialysis of a mixture of solubilized porin Omp32 (0.5% OPOE and 3 mM NaN_3) and micelles of deuterated DM-d67-PC at 35 °C. 10 mM phosphate buffer, pH = 7.4, containing 150 mM NaCl was used for dialysis and in the reference cuvette of the SBSR cell. The spectrum labeled as 0 h was measured immediately after sample injection into the inner sample compartment of the dialysis cell and before starting the flow-through of the dialysis buffer in the outer compartment of the cell. Selected spectra between $t = 0.5$ and 8.2 h demonstrate the progression of dialysis. The last spectrum was measured after $t = 18.7$ h. The 2000 cm^{-1} region of this spectrum was expanded by a factor of 5, to visualize $\nu_{as}(CD_2)$ and $\nu_s(CD_2)$ at 2196 and 2093 cm^{-1} resulting from incorporated deuterated DMPC. Spectra were separated by an absorbance shift of 0.04 AU. Note that the small azide ion (2048 cm^{-1}) is faster extracted than the detergent OPOE (1000 cm^{-1} region). The formation of the porin layer is most clearly documented by the appearance of the amide I and II bands near 1650 and 1540 cm^{-1}. Ge IRE; angle of incidence $\theta = 45°$; number of active internal reflections $N = 14.1 \pm 1$.

in other experiments) solubilized in 0.5% OPOE was filled into the inner compartment of the sample (S) cuvette of the dialysis SBSR cell. The outer chamber contained pure dialysis phosphate buffer, which was not moved during the first measurement started immediately after filling the S-cuvette. The resulting spectrum at $t = 0$ h is shown in Figure 1. Since a SBSR measurement with 1000 scans per sample takes about 20 min, this spectrum reflects an average state of the sample of the first 10 min of dialysis. The band at 2048 cm^{-1} results from the N_3 stretching ($\nu_{as}(N_3)$) of the azide ion. The strong peak at 1082 cm^{-1} and the weaker one at 990 cm^{-1} are vibrations of the detergent OPOE. Small absorbances around 2900 cm^{-1} originated from overlapping vibrations of the methylene groups of detergent and porin, respectively. The two prominent bands in the range between 1700 and 1500 cm^{-1} result from the amide I and amide II vibrations of the protein. The buffer in this SBSR measurement was almost completely compensated, leaving only a small broad band from ν(OH) stretching of H_2O between 3700 and 3060 cm^{-1}. After the first spectrum was acquired, the dialysis buffer was pumped through the outer part of the S-cuvette while the R-cuvette was capped without circulation. The following spectra were recorded at a constant flow rate of buffer of 0.28 mL/min. Typical for the progress of the diffusion/adsorption process is the fast decrease of the intensity of the azide band and the slower vanishing of OPOE bands. This behavior was expected because of the much smaller size of the N_3^- ion compared to the detergent OPOE. The evanescent electric field of the infrared light decreases exponentially with the distance from the surface of the IRE. Thus the absorbance of a substance increases with decreasing distance to the surface of the IRE and reaches a maximum at the surface. Therefore, the appearance of increasing protein bands indicates unambiguously adsorption of Omp32 to the IRE.

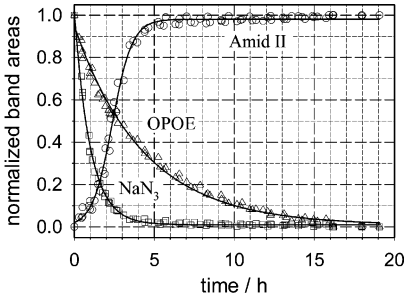

Figure 2. Kinetics of porin adsorption to a Ge IRE, as shown by a plot of normalized band areas of components $A^n(t)$ versus time t. Normalization was performed by setting the largest concentration of each reactant to unity. The selected reactants and bands were NaN_3 at 2048 cm^{-1}, OPOE at 1082 cm^{-1}, and the amide II band of the protein at 1542 cm^{-1}. Data were calculated from two experiments with DMPC and DM-d67-PC, respectively, based on spectra measured with pp and vp polarization. Time courses associated with NaN_3 and OPOE could be fitted with a single-exponential decay according to the following: for NaN_3, $A^n(t) = 0.010 + 1.01e^{(-1.011t)}$ [± 0.017], resulting in a time constant of $\tau = 0.99$ h; for OPOE, $A^n(t) = 0.008 + 0.94e^{(-0.231t)}$ [± 0.024], resulting in a time constant of $\tau = 4.33$ h. No attempt was made to fit the sigmoidal curve associated with porin adsorption to the IRE.

The development of the shape of the amide I band between 1690 and 1600 cm^{-1} shows an intense maximum at 1630 cm^{-1} and a weak shoulder at 1694 cm^{-1}. This is characteristic of a protein rich in antiparallel β pleated sheet structure, an observation which is consistent with data from X-ray crystallography, reporting that 52% of the amino acids are involved in β strands[7] taking the 54 amino acid peptide into account. Parallel to the increase of amide I and amide II bands, a pronounced intensity decrease for ν(OH) occurs. This observation can be explained by the displacement of water in the immediate vicinity of the IRE surface by the growing Omp32 layer on the ATR element in the sample cuvette. The spectrum at the bottom of Figure 1 was measured after the flow-through of the dialysis buffer was stopped (18.7 h). After this time, no further increase of the protein bands could be observed within 1 h. There are weak but unambiguously detectable bands resulting from the stretching vibrations $\nu_{as}(CD_2)$ and $\nu_s(CD_2)$ at 2196 and 2093 cm^{-1} of deuterated DMPC (DM-d67-PC), favoring the conclusion that Omp32 porin adsorption is paralleled by the adsorption of small amounts of phospholipids. Subtracting the spectrum of the Omp32/DM-d67-PC film from the corresponding spectrum of the Omp32/DMPC layer results in a spectrum where the CH stretching vibrations of the protein were compensated and the $\nu_{as}(CH_2)$ and $\nu_s(CH_2)$ bands of DMPC at 2925[1] and 2853 cm^{-1}, respectively, were left. This finding supports the former conclusion and moreover enables the calculation of the amount of DMPC in the layer (see later).

The time-dependent behavior of the components as shown in Figure 2 was evaluated from time-resolved difference spectra, taking the spectrum at the end of dialysis as a reference. The normalized integrated absorbances (band areas) of the azide ion at 2048 cm^{-1}, OPOE at 1082 cm^{-1}, and the protein at 1542 cm^{-1} (amide II) were used. The amide I band overlaps by the bending vibration of bound water, displaced bulk water, and possible slight incompensations of bulk water. Normalization was performed to enable easier comparison of the curves. The largest value of a corresponding band area was set to 1, reflecting the maximum concentrations of 0.5% OPOE and 3 mM NaN_3, or the highest intensity of the amide II band at the end of dialysis, respectively. The decrease of NaN_3 and the detergent could be fitted by a

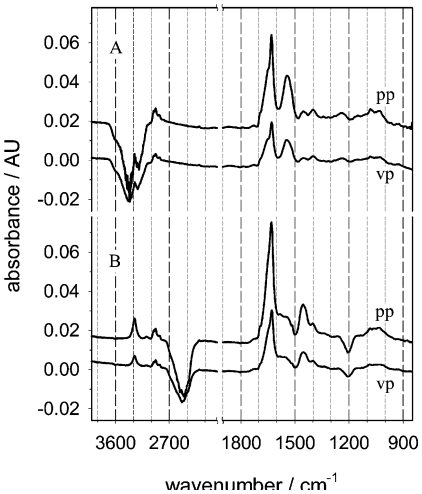

Figure 3. Parallel (pp) and perpendicular (vp) polarized SBSR ATR FTIR absorbance spectra of an Omp32/DM-d67-PC microcrystalline monolayer in an aqueous environment at 23 °C. (A) Spectra recorded after exchange of the dialysis cell by a standard SBSR flow-through cell. Phosphate buffer (10 mM, pH 7.4, 150 mM NaCl in H_2O) was used as the bulk phase in both the sample and reference cuvettes. (B) Spectra of the same porin layer as in (A) starting, however, the measurement after 17 h of contact with the D_2O at 23 °C. Parallel polarized spectra are shifted by 0.02 AU. Ge IRE; angle of incidence $\theta = 45°$; number of active internal reflections $N = 14.1 \pm 1$.

single-exponential function resulting in a time constant for the NaN_3 extraction at 35 °C of $\tau = 0.99 \pm 0.04$ h, whereas the corresponding time constant for OPOE was found to be $\tau = 4.33 \pm 0.05$ h. For comparison, a measurement of the exchange of D_2O against pure H_2O with the same dialysis cell resulted in a time constant of $\tau = 22 \pm 2$ min at 25 °C, where the flow rate of water in the outer compartment was 1.2 mL/min. The time course of the adsorption of Omp32 porin showed a different characteristic. The data could not be fitted satisfactorily by a single-exponential function, since a sigmoidal shape is observed. Within the first hour of dialysis, the amide II band rises more slowly; after about 1 h, however, acceleration is observed, leading into a saturation after about 4 h. The adsorption of Omp32 was almost finished after 5 h. Acceleration of porin adsorption started after about 1.2 h when the OPOE concentration was reduced to ~0.35%. The critical micelle concentration (cmc) of OPOE of ~0.25%[15] was reached after 3 h of dialysis.

After dialysis, the Omp32/lipid film was washed with buffer and the dialysis cap was exchanged by a standard SBSR flow-through cap. During this process, the film was not in contact with buffer for about 10 min. However, it was prevented from complete drying by a thin, visible water layer. The adsorbed porin layer was stable enough to resist this process and succeeding washing procedures with fresh buffer. From now on, all measurements were performed at 23 °C (room temperature) instead of 35 °C used initially during dialysis. The SBSR absorbance spectrum of the porin/lipid layer in H_2O buffer is shown in Figure 3A. Compared to the spectrum at the end of dialysis (Figure 1, 18.7 h), the protein bands have decreased by about 18 ± 2%, as observed by the decrease of the amide II band at 1542 cm^{-1}, the weaker amide III band at 1238 cm^{-1}, and the contributions of the amino acid side chains at 1450 and 1395 cm^{-1}. The displacement of bulk water by the adsorbed layer in the S-compartment of the cuvette leads to negative OH stretching bands near 3400 cm^{-1}. Consequently, there exists also a negative OH bending band at 1645 cm^{-1} masking the behavior of the amide I band. Furthermore, a decrease of approximately 50% of the DM-d67-PC occurred. The OPOE bands at 1082 and 990 cm^{-1} vanished completely or decreased at least to such a low level that the bands could no longer be discriminated from the remaining Omp32 bands in this region. In a typical experiment with unlabeled DMPC, a 27.5 ± 2% reduction of porin was found. We expect that washing of the adsorbed layer and the exchange of the cell cap are the main reasons for this loss, and since the remaining layer was absolutely stable, we suggest that the loss reflects the detachment of loosely bound materials on top of the stable layer of porin and lipid on the Ge plate. A similar behavior was observed in the course of lipid bilayer preparation by means of the LB/vesicle method.[21]

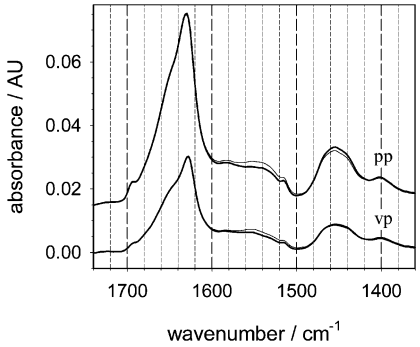

Figure 4. Superimposed parallel polarized (pp) and perpendicular polarized (vp) SBSR ATR FTIR absorbance spectra of the Omp32/DM-d67-PC layer at 23 °C measured at 47 min (thin line) and 17 h (bold line) during H−D exchange. The slow exchange rate of the Omp32 porin protons in this time period is visualized by the decrease of the amide II band at 1542 cm^{-1} and the synchronous increase of the amide II′ band at 1455 cm^{-1}. Ge IRE; angle of incidence $\theta = 45°$; number of active internal reflections $N = 14.1 \pm 1$. Spectra with pp polarization are shifted by 0.015 AU.

Sensing Amide Proton Accessibility by Deuterons: H−D Exchange Measurements. Hydrogen−deuterium (H−D) exchange was initiated by replacing the H_2O phosphate buffer by a 0.15 M NaCl solution in D_2O. SBSR spectra of the porin layer recorded with polarized light are shown in Figure 3B. The negative water bending vibration $\delta(H_2O)$ at 1645 cm^{-1} which overlapped the amide I band (Figure 3A) appears now as $\delta(D_2O)$ at 1206 cm^{-1}. As a consequence, the intensity of the amide I′ band at 1635 cm^{-1} (Figure 3B) is undisturbed by the solvent and reflects the whole amount of the adsorbed Omp32. The amide II′ mode, mainly consisting of the ND in-plane bending vibration, is shifted to 1455 cm^{-1}. A considerable part of the amide protons did not exchange within the 17 h of observation. This is unambiguously documented by the remaining NH stretching band (ν(NH)) at 3280 cm^{-1} resulting from protonated amide groups. Complete replacement of the H_2O-buffer by D_2O was achieved within 7 min using a flow rate of 0.28 mL/min. After about 45 min, the D_2O flow-through was stopped. During the following 17−19 h, a very slow continuation of the exchange of the amide protons could be observed as shown for example for the porin/DM-d67-PC layer spectra in Figure 4. Calculating the surface concentration of Omp32 after about 18 h by means of the remaining ν(NH) band at 3280 cm^{-1} resulted in a value which was about 57% smaller than that obtained via the amide I′ band (see Table 2), suggesting that 43% of the amide protons did not exchange within this time period. Obviously, 43% of the amino acid residues of Omp32 belong to rather rigid structural regions or are hidden within the

Table 2. Quantitative Analysis of Experimental Data

	Omp32/DMPC	*R*	Omp32/DM-d67-PC	*R*
$\int A_{pp}(\tilde{\nu})\, d\tilde{\nu}$ (amide I′)/cm^{-1} [a]	2.349 ± 0.110	1.98 ± 0.13	2.164 ± 0.100	2.03 ± 0.13
$\int A_{vp}(\tilde{\nu})\, d\tilde{\nu}$ (amide I′)/cm^{-1}	1.187 ± 0.055		1.065 ± 0.050	
Γ(Omp32)/(mol·cm^{-2})[b]	$7.78 \times 10^{-12} \pm 1.40 \times 10^{-12}$		$7.11 \times 10^{-12} \pm 1.29 \times 10^{-12}$	
$\int A_{pp}(\tilde{\nu})\, d\tilde{\nu}$ ($\nu_s(CH_2)/\nu_s(CD_2)$)/cm^{-1} [c]	0.0134 ± 0.0020	1.04 ± 0.22	0.0102 ± 0.0040	1.31 ± 0.84
$\int A_{vp}(\tilde{\nu})\, d\tilde{\nu}$ ($\nu_s(CH_2)/\nu_s(CD_2)$)/cm^{-1}	0.0129 ± 0.0019		0.0078 ± 0.040	
Γ(lipid)/(mol·cm^{-2})[d]	$3.8 \times 10^{-11} \pm 0.7 \times 10^{-11}$		$2.6 \times 10^{-11} \pm 1.6 \times 10^{-11}$	
$\int A_{pp}(\tilde{\nu})\, d\tilde{\nu}$ ($\nu_s(CH_2)/\nu_s(CD_2)$)/cm^{-1} (ν(NH))/cm^{-1} [e]	0.769 ± 0.039	1.94 ± 0.14	0.714 ± 0.036	2.01 ± 0.14
$\int A_{vp}(\tilde{\nu})\, d\tilde{\nu}$ (ν(NH))/cm^{-1}	0.397 ± 0.020		0.355 ± 0.018	
Γ (H−Omp32)/mol·cm^{-2} [f]	$3.60 \times 10^{-12} \pm 6.45 \times 10^{-13}$ after 41 min: ≈46%		$3.32 \times 10^{-12} \pm 6.01 \times 10^{-13}$ after 47 min: ≈47%	
$\int A_{pp}(\tilde{\nu})\, d\tilde{\nu}$ (ν(NH))/cm^{-1} [g]	0.718 ± 0.035	1.90 ± 0.13	0.660 ± 0.033	2.06 ±0.15
$\int A_{vp}(\tilde{\nu})\, d\tilde{\nu}$ (ν(NH))/cm^{-1}	0.377 ± 0.019		0.321 ± 0.016	
Γ (H−Omp32)/mol·cm^{-2} [h]	$3.38 \times 10^{-12} \pm 6.03 \times 10^{-13}$ after 19 h: ≈43%		$3.05 \times 10^{-12} \pm 5.56 \times 10^{-13}$ after 17 h: ≈43%	
$\int A_{pp}(\tilde{\nu})\, d\tilde{\nu}$ (ν(NH))/cm^{-1} [i]	0.85 ± 0.08 after 8 min: ≈51%		0.78 ± 0.08 after 8 min: ≈51%	
n(lipid)/*n*(Omp32)[j]	9.2 ± 2.3		8.3 ± 2.1	
Γ(lipid)/Γ(Omp32)[k]	4.9 ± 1.3		3.7 ± 2.3	

[a] Integrated absorbance amide I′, linear baseline 1706−1595 cm^{-1}. [b] Omp32 monomer surface concentration. [c] Integrated absorbance $\nu_s(CH_2)$ and $\nu_s(CD_2)$, linear baseline 2869−2830 and 2131−2045 cm^{-1}. [d] Lipid surface concentration determined by $\nu_s(CH_2)$ and $\nu_s(CD_2)$ absorbance, respectively. [e] Integrated absorbance of ν(NH) (after approximately 45 min contact with D_2O), linear baseline 3400−3200 cm^{-1}. [f] Mean surface concentration of Omp32 monomers reflecting nonexchanged amide protons. These values have to be interpreted as 46% and 47% of nonexchanged amide protons per molecule, after about 45 min of D_2O exposure. [g] Integrated absorbance of ν(NH) (after 17 h (DM-d67-PC) and 19 h (DMPC) contact with D_2O), linear baseline 3400−3200 cm^{-1}. [h] Mean surface concentration of Omp32 monomer reflecting nonexchanged amide protons. These values have to be interpreted as 43% of nonexchanged amide protons per molecule, after 17 h (DM-d67-PC) and 19 h (DMPC) D_2O exposure. [i] Integrated absorbance of ν(NH) (after 8 min D_2O exposure). Up to 8 min, only pp measurements have been performed. Linear baseline 3400−3200 cm^{-1}. [j] Molar lipid-to-protein ratio in the initial solution. [k] Molar lipid-to-protein ratio after porin monolayer formation at the IRE surface.

protein, inaccessible to D_2O. Moreover, within the first 8 min 49% of amide protons exchanged, followed by an additional exchange of about 4% between 8 and 45 min. Between 45 min and about 18 h, it was found that a further 4% of the amide protons were exchanged. It follows that about 8% of the secondary structure exhibits medium flexibility whereas 49% of the amino acids of Omp32 undergo a fast H−D exchange. Consequently, about one-half of the secondary structure exhibits a sufficient flexibility for H−D exchange or a good accessibility to water molecules.

These results are in good agreement with a study of the H−D exchange of a hydrated film of porin OmpF,[33] where kinetics with a fast, an intermediate, and a very slow exchange rate exhibiting time constants in the range of 1.3 min, 28 min, and 94 h have been reported.

In the region of the amide II band at ∼1540 cm^{-1}, there exist additional absorption bands of amino acid side chains. We assigned tentatively the band at 1583 cm^{-1} to the asymmetric stretching vibration $\nu_{as}(COO^-)$ of carboxylate groups (aspartic and glutamic acid residues) and the band at 1515 cm^{-1} to an aromatic ring vibration of tyrosine, consisting of $\nu(C-C)_{ring}$ and δ(CH).[34]

Calculation of Surface Concentrations. Quantification of porin, DMPC, and DM-d67-PC in adsorbed films has been performed using the spectra measured after 17−19 h of H−D exchange. Surface concentrations were calculated by means of eq 9 from measurements with parallel and perpendicular polarized incident light, using the amide I′ band for Omp32 and the symmetric stretching vibration of the methylene groups ($\nu_s(CH_2)$ and $\nu_s(CD_2)$) for DMPC or DM-d67-PC, respectively. The results are summarized in Table 2.

The mean surface concentration of Omp32 adsorbed to the Ge plate was $\Gamma = 7.45 \times 10^{-12} \pm 1.45 \times 10^{-12}$ mol·cm^{-2}. Assuming a protein monolayer, this corresponds to an area per molecule of 22.3 ± 4.3 nm^2 or to a packing density of one Omp32 trimer per 67 ± 13 nm^2. To compensate the contribution of Omp32 to symmetric CH_2 stretching ($\nu_s(CH_2)$) of DMPC, we have subtracted the spectra of Omp32/DM-d67-PC from the spectra of Omp32/DMPC. A scaling factor Γ(Omp32/DMPC)/Γ(Omp32/DM-d67-PC) = 1.09 took account of the different protein surface concentrations achieved with these two experiments; see Table 2.

DMPC consists of 28 CH_2 groups; however, only $\nu = 26$ were considered in DM-d67-PC in eq 9 because two nondeuterated methylene groups of the glycerin part had to be taken into account. The resulting surface concentrations resulted in $\Gamma = 3.8 \times 10^{-11} \pm 0.7 \times 10^{-11}$ mol·cm^{-2} for DMPC and $\Gamma = 2.6 \times 10^{-11} \pm 1.6 \times 10^{-11}$ mol·cm^{-2} for DM-d67-PC. The resulting lipid to Omp32 ratio (L/P) resulted in values within 2−6 (mol/mol). The initial L/P ratio of the solutions was 2−3 times higher. All results are summarized in Table 2.

Orientation Analysis. Dichroic difference spectra D^* as described in the Theoretical Section were used to assess the orientation of the Omp32 layer. As mentioned, the isotropic dichroic ratio R_{iso} depends on the angle of incidence and the refractive indices of the IRE, as well as on the optical constants of the film and the bulk phase. Refractive indices of $n_2 = 1.45 \pm 0.06$ for the adsorbed layer and $n_3 = 1.32 \pm 0.06$ were used in the D_2O environment. The value of the isotropic dichroic ratio in the amide I′ region of a porin layer turned out to be $R_{iso} = 1.65 \pm 0.25$. Thus the dichroic difference spectra of the Omp32/DM-d67-PC in the amide I′ region were calculated with $R_{iso} = 1.65$, as well as with $R_{iso} = 1.4$ and $R_{iso} = 1.9$. The results are presented in Figure 5.

First, distinctly marked dichroic effects can be noticed in the amide I′ region. Independent of the correct value of R_{iso} within the range of uncertainty, a small positive band at 1695 cm^{-1} and an intense positive band at 1635 cm^{-1} are significant. While the small band at 1695 cm^{-1} is also visible in the original SBSR absorbance spectra (Figure 5, top), the D^* band at 1635 cm^{-1}, however, is significantly shifted with respect to the main peak in the

(33) Abrecht, H.; Goormaghtigh, E.; Ruysschaert, J.-M.; Homblé, F. *J. Biol. Chem.* **2000**, *275*, 40992−40999.
(34) Barth, A. *Prog. Biophys. Mol. Biol.* **2000**, *74*, 141−173.

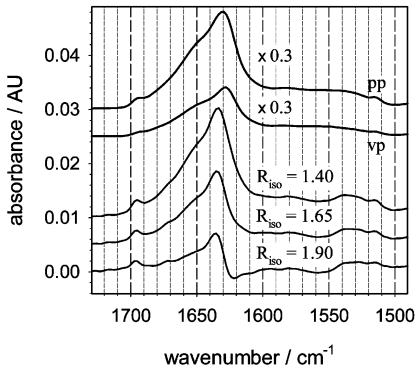

Figure 5. Dichroic difference spectra $D^* = A_{pp} - R_{iso}A_{vp}$ from the Omp32/DM-d67-PC monolayer using the calculated isotropic dichroic ratio for the amide I′ region $R_{iso} = 1.65$ and the associated limits of about 95% confidence $R_{iso} = 1.40$ and $R_{iso} = 1.90$, respectively. The underlying SBSR absorbance spectra (A_{pp}, A_{vp}), measured with parallel (pp) and perpendicular (vp) polarized incident light are shown on top (scaled down by a factor of 0.3). For the sake of presentation, D^* with $R_{iso} = 1.65$ is shifted by 5 mAU, D^* with $R_{iso} = 1.40$ is shifted by 10 mAU, and A_{vp} and A_{pp} are shifted by 25 and 30 mAU, respectively. Optical parameters are as in Figure 4.

original absorbance spectra which is at 1630 cm^{-1}. Obviously, this frequency results from a superposition of the component near 1635 cm^{-1} with a second component at 1623 cm^{-1} as revealed by the shape of the D^* spectra obtained with $R_{iso} = 1.65$ and $R_{iso} = 1.90$. As a consequence, one can conclude that the mean transition moment associated with 1635 cm^{-1} is predominantly inclined toward to the normal to the IRE (*z*-axis), that is, must form an angle within 54.7° and 0°, while the mean transition moment corresponding to 1623 cm^{-1} must assume an angle within 54.7° and 90°. According to the underlying model of a LCU, the transition moments of both conformational populations are assumed to exhibit isotropic arrangement around the *z*-axis.

At least two additional positive components can be detected by the D^* spectra. The first is visible at 1672 cm^{-1}, and the second appears as a broad band in the region of 1650 cm^{-1}.

Discussion

A procedure applied for two-dimensional crystallization of membrane proteins[17] could be successfully adapted for use with ATR IREs. The procedure described in this paper leads to well-oriented monolayers of Omp32, where each protein monomer is associated with 2−6 lipid molecules. The observation of a saturation in the course of Omp32 adsorption strongly suggests that a monolayer is formed (Figure 2). Moreover, distinct dichroic phenomena (Figure 5) give evidence for an Omp32/DMPC assembly forming a uniaxially ordered layer. This finding is consistent with electron microscopic data obtained from OmpF/DMPC layers prepared by the same method.[15] The very slow increase of the amide II absorbance at elevated time after 5 h (Figure 2) can be explained by the adsorption of loosely bound Omp32 aggregates to the stable monolayer, since these aggregates turned out to be easily eliminated by rinsing the flow-through cuvette with pure buffer, while the magnitude of amide II absorbance detected within the first 5 h remained stable.

Omp32/DMPC and Omp32/DM-d67-PC layers resulted in a mean area per Omp32 trimer of 67 ± 13 nm^2. This finding is in good agreement with electron microscopical studies of 2D crystals from Omp32 (space group *p*312), which were produced by the conventional dialysis technique[18] and showed a trimer area of 87 nm^2 and a DMPC-to-trimer ratio of 6. Figure 6 shows the averaged projection structure from an electron micrograph of this kind of crystal, illustrating the assembly and orientation of porin trimers. In addition, Omp32 exists in two 3D crystal forms.[7] The one with the smaller unit cell size (CF2) exhibits a lateral arrangement leading to an area per trimer of 67 nm^2 which fits exactly our mean area.

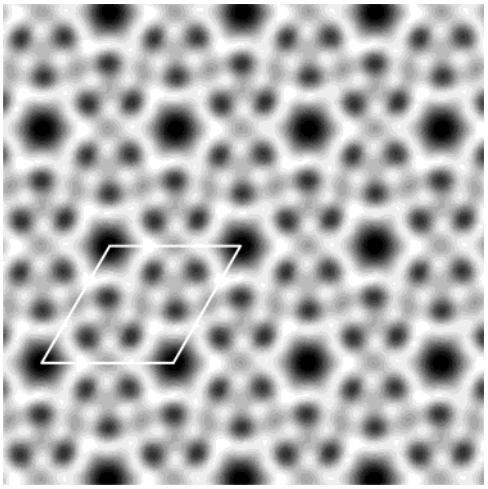

Figure 6. Correlation average of an electron micrograph from a two-dimensional crystal of isolated Omp32. The specimen was negatively stained with uranyl acetate. Black areas indicate pores and holes filled with stain, and bright areas indicate biological material, i.e., protein. The space group is *p*321 with a unit cell containing two trimers in opposite orientation with respect to the membrane plane. The symmetry was determined by decoration experiments. The unit cell is marked and has a size of $a = b = 13.5$ nm, enclosing an angle of $\gamma = 120°$.

It is known from X-ray crystallography that in the case of OmpF the mean angle between the β-strands and the barrel axis corresponds to ∼45°.[35] The value calculated for Omp32 in the same manner as given in ref 35 is approximately 42° (unpublished results), being very close to the theoretical value for an ideal 16 stranded β-barrel. This calculation does not include possible but unknown contributions from the associated peptide. The high-frequency component of the antiparallel β-sheet in the amide I band is reported to be oriented in the direction of the β-strand, whereas the low-frequency component is oriented approximately perpendicular to the strand direction.[36,37] From this constellation, one could expect mean orientations of the transition moments of both vibrations forming angles close to 45° with the normal to the IRE (*z*-axis). Taking these values for Omp32 and assuming a nontilted β-barrel axis, the dichroic ratio for a vibration with a transition moment pointing in the strand direction, as well as perpendicular to it, can be calculated by means of eq 1 to be $R = 2.42$, using the same optical parameters as for the calculation of R_{iso} (for theoretical details, the reader is referred to ref 30, eq 130).

Indeed, we observed positive components in the dichroic difference spectra (D^*). Moreover, NH stretching at 3280 cm^{-1} resulted in a dichroic ratio of $R = 2.01 \pm 0.14$ (Table 2) ($R_{iso} = 1.66$ at 3280 cm^{-1}) thus forming an angle of 49.6° ± 4.3° (using $n_3 = 1.28$ according to ref 26) with the normal to the IRE. Assuming this transition moment to be directed along the NH bond would support the model of

(35) Páli, T.; Marsh, D. *Biophys. J.* **2001**, *80*, 2789−2797.
(36) Chirgadze, Y. N.; Nevskaya, N. A. *Biopolymers* **1976**, *15*, 607−625.
(37) Kubelka, J.; Keiderling, T. A. *J. Am. Chem. Soc.* **2001**, *123*, 6142−6150.

two-dimensional microcrystals with barrel axes near normal to the IRE surface. However, near 1623 cm^{-1} there is a distinct negative D^* band which could also be assigned to the intense low-frequency component of the antiparallel β-sheet. In this case, however, no obvious consistence with the suggested model would exist. Future experiments and theoretical considerations have to give more detailed information with respect to the assignment and the direction of transition moments of the vibrations detected at 1630 and 1623 cm^{-1}.

In this paper, we have described a procedure enabling the preparation of a stable oriented monolayer of Omp32 on an ATR crystal. Therefore, a principal prerequisite for the study of electric field dependent channel gating by electric field modulated excitation spectroscopy is fulfilled. Experiments using a setup as presented in ref 38 are in progress.

Acknowledgment. This work was supported by a grant (Na 226/9-2) from the Deutsche Forschungsgemeinschaft (DFG). M.S. thanks the DFG for a PhD scholarship. P. Lasch is kindly acknowledged for helpful discussions. We thank Alain Messinger from Messinger Membrane Systems, Technopark, CH-8005 Zurich, for supplying adequate dialysis membranes.

(38) Fringeli, U. P.; Baurecht, D.; Günthard, Hs. H. In *Infrared and Raman Spectroscopy of Biological Materials*; Gremlich, H. U., Yan, B., Eds.; Marcel Dekker: New York, 2000; pp 143−192.

Abbreviations

FTIR	Fourier transform infrared
ATR	attenuated total reflection
IRE	internal reflection element
DMPC	1,2-dimyristoyl-*sn*-glycero-3-phosphocholine
DM-d67-PC	1,2-dimyristoyl-d67-*sn*-glycero-3-phosphocholine
OPOE	*n*-octylpolyoxyethylene
SBSR	single beam sample reference
cmc	critical micellar concentration
L/P	lipid-to-protein ratio
LCU	liquid crystalline ultrastructure
LB	Langmuir−Blodgett

LA034153M